

Valley Phase and Voltage Control of Coherent Manipulation in Si Quantum Dots

Neil Zimmerman^{1*}, Peihao Huang^{1,2}, Dimitrie Culcer^{†3}

¹Quantum Measurement Division, National Institute of Standards and Technology, MD 20899, USA

²Joint Quantum Institute, University of Maryland and National Institute of Standards and Technology, MD 20742, USA and

³School of Physics, The University of New South Wales, Sydney 2052, Australia

With any roughness at the interface of an indirect-bandgap semiconducting dot, the phase of the valley-orbit coupling can take on a random value. This random value, in double quantum dots, causes a large change in the exchange splitting. We demonstrate a simple analytical method to calculate the phase, and thus the exchange splitting and singlet-triplet qubit frequency, for an arbitrary interface. We then show that, with lateral control of the position of a quantum dot using a gate voltage, the valley-orbit phase can be controlled over a wide range, so that variations in the exchange splitting can be controlled for individual devices. Finally, we suggest experiments to measure the valley phase and the concomitant gate voltage control.

The physics of valleys in Si is complicated, both theoretically and experimentally. On the theory side, calculations of the effects of valleys, especially with rough interfaces, often requires very large atomistic simulations; those simulations can sometimes make it more difficult to achieve a simple, intuitive understanding of the underlying physics. In this paper, we present a very simple and intuitively-appealing framework to understand and calculate the effect of the phase of the complex valley-orbit coupling in devices with rough interfaces. On the experimental side, the effects of the valleys can be bound up with spin and orbital effects, thus making effective classical and coherent control of the devices more challenging. We propose a simple experimental method (lateral gate voltages) to both analyze and to control these confounding experimental effects when they arise from the complex phase.

Quantum coherent manipulation of electrons in Si has been a very active field of study recently[1][2]. The advantages of Si include low spin-orbit coupling and the ability to isotopically enrich ²⁸Si, both of which will tend to reduce the decoherence of spin qubits. In addition, the integration with CMOS classical circuitry holds the potential for monolithically integrating qubits with control circuits[2]. Very recent advances in demonstrating quantum coherence include driving single spins in SiGe quantum dots with micromagnets[3][4], single spins in Si/SiO₂ quantum dots including Stark-shifted addressability[5], and a two-qubit gate in Si/SiO₂ quantum dots[6].

One complication for quantum control in Si is engendered by the valley degree of freedom; there are six equivalent positions in the three-dimensional band structure[1]. Because there is no external control of the valley quantum number, complications include difficulty

in well-defined initialization and enhanced spin decoherence at valley relaxation “hotspots”[7]. Experimental measurements of the magnitude of the valley splitting between the lowest two valley states include spin-valley “hotspots”[8] and valley splitting magnitude tunable with electric field[7][9]. The experimental work most relevant for our study is Shi et al[10], which showed experimentally a shift in the single-triplet splitting J for two electrons *on a single dot*, where J is dominated by the energy difference between single-particle ground and excited valley-orbit states in Si/SiGe. In particular, they measured J as a function of lateral shift using gate voltages; they showed about a 20 % shift, and interpreted it as coming from the change in single-particle valley-orbit energies arising from a rough interface (they solved this for the toy model of a single atomic step).

In the vicinity of an interface, the lowest energy valleys are typically perpendicular to the interface, and are split by the valley-orbit coupling, which is defined as

$$\Delta = \langle z | (\mathcal{V} + eFz) | \bar{z} \rangle, \quad (1)$$

where $|z\rangle$, $|\bar{z}\rangle$ are the bare valley states centered at $k_z = \pm k_0 = \pm(0.85)2\pi/a_0$, \mathcal{V} is the interfacial potential energy, F is the applied electric field, and a_0 is lattice constant; this leads to eigenstates which are symmetric superpositions of $|z\rangle$ and $|\bar{z}\rangle$ (see text above Eqn 7), split by $|\Delta|$. We note that, by virtue of the definition, the coupling is a complex quantity $\Delta = |\Delta|e^{i\phi}$.

Theoretical predictions of the valley-orbit coupling include predictions of magnitude in perfect SiGe[11][12][13][14] and SiO₂[15][16], magnitude in disordered interfaces[17][18][19], effects of valley phase on magnitude[20][21][22], spin-valley interactions[23][24] and intervalley dynamics at interface steps[25].

In contrast to the magnitude, there has been somewhat less consideration of the complex phase[20][21][22][15] ϕ . In terms of the effect of interface roughness on tunneling, Shiau et al [26] used an atomistic tight-binding model to calculate, among other quantities, the intra- and inter-valley tunneling matrix elements, between lead and dot,

*+1-301-975-5887; neilz@mailaps.org;
ftp://ftp.nist.gov/pub/physics/neilz/papers.html
†d.culcer@unsw.edu.au

as a function of atomic step position and miscut angle; they also briefly discussed the significance of the valley phase in preserving valley index under tunneling. Similarly, Gamble et al [18] used a semianalytical expansion in disorder matrix elements to calculate, among other quantities, the intervalley matrix element, between two dots, as a function of atomic step position.

Although the global phase ϕ for a single quantum dot or donor has no physical consequence, the phase difference $\Delta\phi$ between two quantum dots or donors has great significance, because matrix elements (such as exchange splitting[22] and preservation of valley index [26]) between the two dots depend on $\Delta\phi$. As in studies of the magnitude of the valley splitting, the roughness of the interface is the crucial device feature; this is because the Bloch wavefunction is tied to the Si lattice, while the envelope of the electron wavefunction follows the rough interface. With $d = a_0/4$ the thickness of a single terrace step, $2k_0d \approx 2(0.85)(2\pi/a_0)(a_0/4) \approx 0.42(2\pi)$ [ref[20]]. Thus, not only is the value of ϕ large, it is also incommensurate with 2π ; this basic fact is the origin of the large effects discussed in this paper.

The main point of this paper is to present a simple analytic approach to estimating the effects of interface roughness on qubit gate operation frequencies through $\Delta\phi$ and J . We do this by focussing on the valley phase as an intermediary to calculate the exchange energy for two electrons in two quantum dots. This occurs because, as we will show, the exchange splitting $J \propto 1 + \cos \Delta\phi$. Thus, the large value of $\Delta\phi$ manifests itself as a large effect on the σ_z rotation frequency (J/h) for both two electrons on two dots (2e2d) singlet-triplet qubits and the two-qubit gate coupling frequency (J/h) for 2e2d single spin qubits; as we will show, these effects are present for both interfaces with steps (corresponding to Si/SiGe) and with random fluctuations (Si/SiO₂).

In this paper, we will show (within the effective mass approximation) i) the derivations of $\Delta\phi$ based on interface roughness and the dependence of J on $\Delta\phi$, ii) results of simulations of $\Delta\phi$ for both step and random interfaces, and iii) the ability to control the coupling phase with applied gate voltage, by laterally shifting quantum dots. *We emphasize that, in contrast to previous results[26][18] where tunneling matrix elements have been obtained for some particular interface roughnesses, the power of the present work is combining the focus on the valley phase with the resulting very simple analytical method to calculate the effect on tunneling and valley index preservation of any arbitrary interface roughness.* For comparison, we note that a full atomistic calculation for a single dot typically requires 1 million atoms and at least 10 orbitals per atom[27]; in addition, for multiple dots, the number of atoms would increase substantially to take into account both the additional dots and the large volume between the dots.

We consider two electrons, one in each of two quantum dots (L and R denote the two lateral locations of the quantum dots), localized in the z-direction by the

combination of interface and accumulation gate voltage, and localized in the x-, y-directions by lateral gates. For each dot, the potential is then

$$V_L(x, y, z) = \frac{\hbar^2}{2m^*a^2} \left[\frac{(x - x_L)^2 + y^2}{a^2} \right] + \mathcal{V}(x, y, z) + eFz, \quad (2)$$

and similarly for position R. The QD has a Fock-Darwin radius a , with m^* the Si in-plane effective mass. The effective mass (EMA) single-electron wavefunction for a multi-valley system (left dot L and valley z) is

$$L_z(x, y, z) = \phi_L(x, y) \psi(z) u_z(\mathbf{r}) e^{ik_0z}, \quad (3)$$

and similarly for position R and valley \bar{z} ; here, $\psi(z)$ is the envelope function for the z -direction and $u_z(\mathbf{r})$ has the periodicity of the lattice. Then, in the absence of valley-orbit coupling, the lowest orbital state is

$$\phi_L(x, y) = \frac{1}{a\sqrt{\pi}} e^{-\frac{(x-x_L)^2+y^2}{2a^2}}, \quad (4)$$

and similarly for position R.

Finally, the interface potential is

$$\mathcal{V}(x, y, z) = U_0 \theta[\zeta(x, y) - z], \quad (5)$$

where $\zeta(x, y)$ is the height of the rough interface. With this interface, we make the assumption that the center-of-charge of the wavefunction follows exactly: $\psi(z) \rightarrow \psi(z - \zeta)$. This assumption is justified when the variation of $\zeta(x, y)$ with respect to x, y is not too large (see Supplement). Combining this with Equations 1, 3, 5, we obtain

$$\Delta_D \approx \Delta_0 \int_{-\infty}^{\infty} \int_{-\infty}^{\infty} dx dy |\phi_D(x, y)|^2 e^{-2ik_0\zeta(x, y)}, \quad (6)$$

where Δ_0 is the valley splitting in the absence of interface roughness. Equation 6 is simple and appealing: It shows a simple analytical connection between the interface roughness $\zeta(x, y)$ and the valley phase[20]. This simple result depends crucially on only two assumptions: i) the electron wavefunction locally follows the rough interface (Supplement A. through C., including particularly an analysis based on comparing kinetic energy cost to potential energy gain); ii) the electron wavefunction contains approximately only the ground orbital state (Supplement D).

Finally we define $\Delta_{L,R} = |\Delta_{L,R}| e^{-i\phi_{L,R}}$ and $\Delta\phi = \phi_L - \phi_R$. We note that the assumption of pure position states L and R is equivalent to assuming the Coulomb repulsion energy is large compared to the tunneling energy, which is generally experimentally valid. A simple consequence of Equation 6: If we consider a flat interface with one step of height d located between the two dots, because ζ is defined with respect to the underlying Si lattice, $\Delta\phi = 2k_0d$, as discussed above.

We now turn to the dependence of exchange energy on valley phase: After mixing $|z\rangle$ and $|\bar{z}\rangle$ through the

valley splitting, the single-particle states are $|L_{\pm}\rangle = \frac{1}{\sqrt{2}}(|L_z\rangle \pm e^{i\phi_L}|L_{\bar{z}}\rangle)$, and similarly for R. Thus, the tunneling matrix element between lowest-lying states $t_{--} = t_{++} = \langle L_-|T|R_- \rangle$ is

$$\begin{aligned} t_{--} &= \frac{1}{2}(\langle L_z| - e^{-i\phi_L}\langle L_{\bar{z}}|)T(|R_z\rangle - e^{i\phi_R}|R_{\bar{z}}\rangle) \\ &= \frac{1}{2}[\langle L_z|T|R_z\rangle + e^{-i\Delta\phi}\langle L_{\bar{z}}|T|R_{\bar{z}}\rangle] = \frac{t_0}{2}[1 + e^{-i\Delta\phi}], \end{aligned} \quad (7)$$

where T and t_0 are the tunneling Hamiltonian and the tunneling matrix element in the absence of valley effects, respectively. Similarly, $t_{-+} = \frac{t_0}{2}[1 - e^{-i\Delta\phi}]$. The exchange energy $J = 4|t_{--}|^2/U$, where U is the on-site repulsion energy, is thus

$$J = \frac{J_0}{2}(1 + \cos \Delta\phi), \quad (8)$$

where $J_0 = 4|t_0|^2/U$ is the exchange energy in the absence of valley phase.

Figure 1 shows the results for simulated SiGe interfaces (horizontal sections separated by vertical steps) for both random (approximately equal numbers of upgoing and downgoing steps) and for vicinal (all steps are upgoing) interfaces. The interfaces were generated by assigning steps at random lateral positions so as to get a particular average lateral density, as indicated in the graphs. As shown, for any roughness, $\Delta\phi$ is of large magnitude compared to 2π , and has no systematic dependence on tilt or randomness; these facts both occur because, as discussed above, $2k_0d$ is large for a single terrace step.

Similar to Figure 1, Figure 2 shows the calculation for $\Delta\phi$ appropriate for a Si/SiO₂ interface without and with vicinal tilt. We generated this interface by i) first generating a random Fourier transform of variable width $\Delta\lambda$, ii) inverse Fourier transforming, and then iii) scaling to give a total vertical height of about 1.5 nm (equivalent to the height of 10 random steps in Figure 1a). In Figure 2a), zero width corresponds to a single correlation length of 20 nm (sinusoidal roughness), and the largest width $\Delta\lambda = 100$ corresponds to a range of correlation lengths between two and 20 nm. Previous high resolution TEM and weak localization studies of the Si/SiO₂ interface have yielded a range of correlation lengths from a few nm[28] up to 100 nm[29][30]. We see that, as for the SiGe interface, vicinal and non-vicinal randomness with a variety of correlation lengths all lead to large values of $\Delta\phi$.

We now turn to considering an experimental control of $\Delta\phi$ and J , using gate voltages. Since the valley phase in Equation 6 arises from the vertical height of the interface, at first glance one might think that moving the dot vertically into the Si substrate might have a strong effect on $\Delta\phi$; although a vertical electric field has strong effect on the magnitude of the coupling^{[9]–[21]}, it has a small effect on $\Delta\phi$ [15], at least for a flat interface. However, due to the strong dependence of the valley phase on the exact local realization of the interface roughness, using

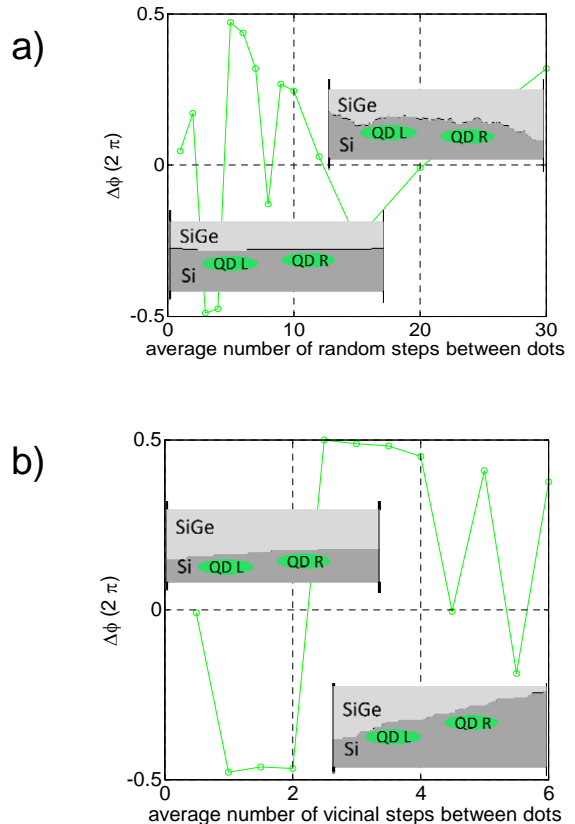


FIG. 1: Calculation of $\Delta\phi$ for Si/SiGe interfaces (horizontal sections separated by vertical steps), for two types of simulated interfaces: a) Interface is on average horizontal, and contains upgoing and downgoing steps randomly distributed with a lateral density as indicated; b) Interface is tilted (vicinal), with only upgoing steps randomly distributed as indicated. Insets are sketches of representative interfaces at the two ends of the ranges of lateral densities. Note that $\Delta\phi$ is large for all rough interfaces, because $2k_0 a_0/4$ is large.

a gate voltage to shift the dot laterally can have a large effect.

Overall, Figure 3 shows this possibility: the upper panel shows the effect on $\Delta\phi$ of using a lateral gate voltage to move both dots laterally with a constant separation, for both a sinusoidal interface ($\Delta\lambda = 0$) and random interface ($\Delta\lambda = 10$). Clearly, the phase difference $\Delta\phi$ and the concomitant energies are strong functions of the lateral position; this is simply because moving a dot changes the local interface height, and thus the phase factor in Equation 6. The lower panel shows the concomitant effect on the tunneling matrix elements and on the exchange energy. While the specific gate voltage dependence is likely impossible to predict in advance, this Figure shows that there is the hope of operationally controlling qubit gate frequencies; this experimental control does not depend on our simple analytical framework[26][18]. In comparing Figure 3 to Figures 1

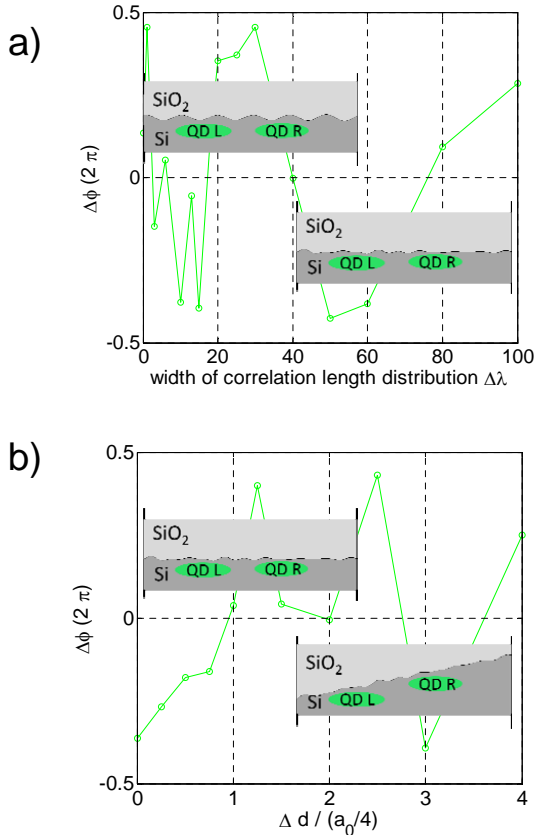


FIG. 2: Calculation of $\Delta\phi$ for Si/SiO₂ interfaces: a) Interface is on average horizontal, and is generated by inverse Fourier transform of a randomly generated function of variable width. Larger width yields a more random interface, as indicated by the inset sketches. b) Similar to a), using a single random interface and a variable amount of vicinal tilt; Δd is the vicinal height difference between the two dots, so that $\Delta d/(a_0/4)$ is the height difference in units of equivalent terrace steps (compare to Figure 1). Note that the interface is not flat at the left end of both graphs, so that $\Delta\phi$ is nonzero there.

and 2, we note that the systematic appearance of Figure 3 relies on the fact that the interface in that Figure has a correlation length approximately equal to the total range of 20 nm, so that the random structure in $\Delta\phi$ apparent in Figures 1 and 2 only appears over the total range of separation in Figure 3.

How can we test the complex valley phase experimentally? First of all, it appears that the global phase (i.e., ϕ_L) is not measurable, because there is no physical realizable corresponding to it. We suggest two possible experiments for testing $\Delta\phi$ directly: i) Measurements of the exchange energy splitting J (references [31][32]) in a DQD could be done as a function of multiple lateral gate voltages in the same way as described above. If J changes in a systematic way with the lateral position of both dots, this would indicate the likelihood of valley phase-mediated modulation of J ; ii) Very recently, valley blockade in a

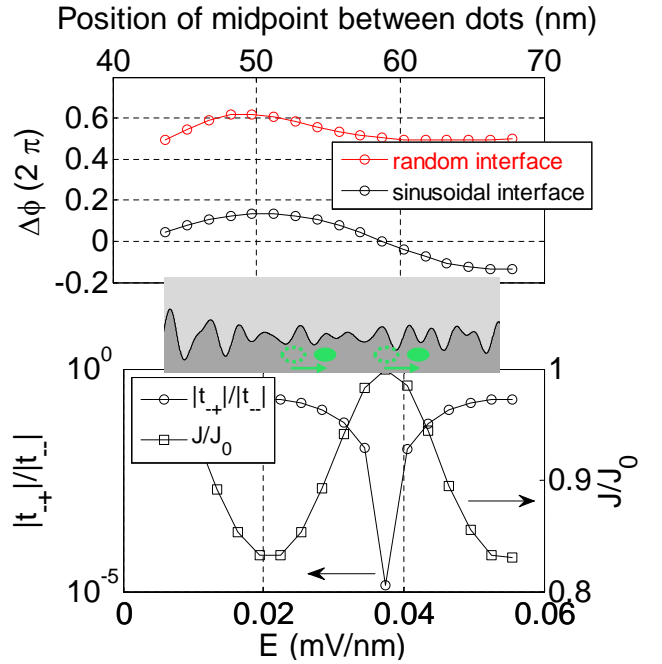


FIG. 3: Using lateral gate voltages to control $\Delta\phi$ and J by moving one or both quantum dots. Lower panel: J and t_{\pm} are from sinusoidal interface result in upper plot. In this simulation, the separation between the dots is held fixed, to maintain the bare tunneling energy t_0 as a constant. Lateral electric field values are estimated for a parabolic confining potential that would yield a quantum dot of orbital size 60 nm and energy spacing 1 meV

double quantum dot (DQD), exactly analogous to Pauli spin blockade[33][34][31]), has been reported[35]. In this work, an asymmetry in the size of the bias triangles in a DQD is attributed to blockade in one bias direction due to the impossibility of inter-valley tunneling. Such valley blockade depends on $\Delta\phi = 0$, and thus the leakage current in the blocked region $I_{\text{leak}} \propto (1 - \cos \Delta\phi)/2$. Thus, we suggest examining the leakage current magnitude as a function of lateral gate voltage.

Also, we estimate as insignificant the magnitude of spin dephasing (through the dependence of J on $\Delta\phi$) due to charge noise which would modulate the lateral position of one or both dots: From Figure 3, $dJ/dx \approx 0.1J_0/(10 \text{ nm})$, lateral motion $dx/dV_G \approx (1 \text{ nm}/10 \text{ mV})$, and a voltage noise magnitude $\Delta V_G = 1 \mu\text{V}$, we obtain the noise magnitude $\Delta J \approx 10^{-6}J_0$. Finally, one way of suppressing the complex valley phase effects and of increasing the valley splitting magnitude, would be to make devices with perfectly flat atomically sharp terraces as large as $10 \mu\text{m}$ [36][37]. However, it is likely that subsequent growth of SiO₂ or SiGe will lead to substantial roughening of such terraces, and thus it appears likely that these valley phase effects will still be present in typical quantum coherent devices.

It is a pleasure to acknowledge useful discussions with Josh Pomeroy, Mark Stiles, Michael Stewart Jr (all of

NIST), Andras Palyi (BUTE), John Gamble (Sandia) and Chris Richardson (LPS).

-
- [1] F. A. Zwanenburg et al., *Rev. Mod. Phys.* **85**, 961 (2013).
- [2] J. J. L. Morton, D. R. McCamey, M. A. Eriksson, and S. A. Lyon, *Nature* **479**, 345 (2011).
- [3] P. Scarlino et al., *Phys. Rev. Lett.* **115**, 106802 (2015).
- [4] E. Kawakami et al., *Nature Nanotech.* **9**, 666 (2014).
- [5] M. Veldhorst et al., *Nature Nanotech.* **9**, 981 (2014).
- [6] M. Veldhorst et al., *Nature* **526**, 410 (2015).
- [7] C. H. Yang et al., *Nature Comm.* **4**, 2069 (2013).
- [8] X. Hao et al., *Nature Comm.* **5**, 3860 (2014).
- [9] S. Goswami, K. A. Slinker, M. Friesen, L. M. McGuire, J. L. Truitt, C. Tahan, L. J. Klein, J. O. Chu, P. M. Mooney, V. W. van der Weide, et al., *Nature Physics* **3**, 41 (2007).
- [10] Z. Shi et al., *Appl. Phys. Lett.* **99**, 233108 (2011).
- [11] T. B. Boykin, G. Klimeck, M. A. Eriksson, M. Friesen, S. N. Coppersmith, P. von Allmen, F. Oyafuso, and S. Lee, *Applied Physics Letters* **84**, 115 (2004), URL <http://scitation.aip.org/content/aip/journal/apl/84/1/10.1063/1.1637718>; `jsessionid=eQPbre3FvIyOPAdejAVTNIWa.x-aip-live-03`.
- [12] T. B. Boykin, G. Klimeck, M. Friesen, S. N. Coppersmith, P. von Allmen, F. Oyafuso, and S. Lee, *Phys. Rev. B* **70**, 165325 (2004), URL <http://link.aps.org/doi/10.1103/PhysRevB.70.165325>.
- [13] T. B. Boykin, N. Kharche, and G. Klimeck, *Phys. Rev. B* **77**, 245320 (2008), URL <http://link.aps.org/doi/10.1103/PhysRevB.77.245320>.
- [14] M. Friesen and S. N. Coppersmith, *Phys. Rev. B* **81**, 115324 (2010), URL <http://link.aps.org/doi/10.1103/PhysRevB.81.115324>.
- [15] A. L. Saraiva, M. J. Calderón, X. Hu, S. Das Sarma, and B. Koiller, *Phys. Rev. B* **80**, 081305 (2009), URL <http://link.aps.org/doi/10.1103/PhysRevB.80.081305>.
- [16] A. L. Saraiva, M. J. Calderón, R. B. Capaz, X. Hu, S. Das Sarma, and B. Koiller, *Phys. Rev. B* **84**, 155320 (2011), URL <http://link.aps.org/doi/10.1103/PhysRevB.84.155320>.
- [17] S. Srinivasan, G. Klimeck, and L. P. Rokhinson, *Applied Physics Letters* **93**, 112102 (2008), URL <http://scitation.aip.org/content/aip/journal/apl/93/11/10.1063/1.2981577>; `jsessionid=eQPbre3FvIyOPAdejAVTNIWa.x-aip-live-03`.
- [18] J. K. Gamble, M. A. Eriksson, S. N. Coppersmith, and M. Friesen, *Phys. Rev. B* **88**, 035310 (2013), URL <http://link.aps.org/doi/10.1103/PhysRevB.88.035310>.
- [19] D. Culcer et al., *Phys. Rev. B* **82**, 205315 (2010).
- [20] M. Friesen, S. Chutia, C. Tahan, and S. N. Coppersmith, *Phys. Rev. B* **75**, 115318 (2007), URL <http://link.aps.org/doi/10.1103/PhysRevB.75.115318>.
- [21] M. Friesen, M. A. Eriksson, and S. N. Coppersmith, *Applied Physics Letters* **89**, 202106 (2006), URL <http://scitation.aip.org/content/aip/journal/apl/89/20/10.1063/1.2387975>; `jsessionid=e8uHB9fAyj0HD4RgKZM7PzA+.x-aip-live-03`.
- [22] Y. Wu and D. Culcer, *Phys. Rev. B* **86**, 035321 (2012), URL <http://link.aps.org/doi/10.1103/PhysRevB.86.035321>.
- [23] D. Culcer et al., *Phys. Rev. B* **82**, 155312 (2010).
- [24] W. Huang, M. Veldhorst, N. M. Zimmerman, A. S. Dzurak, and D. Culcer, *Phys. Rev. B* **95**, 075403 (2017).
- [25] P. Boross, G. Szchenyi, D. Culcer, and A. Plyi, *Phys. Rev. B* **94**, 035438 (2016).
- [26] S. yuan Shiao, S. Chutia, and R. Joynt, *Phys. Rev. B* **75**, 195345 (2007).
- [27] R. Rahman, E. Nielsen, R. P. Muller, and M. S. Carroll, *Phys. Rev. B* **85**, 125423 (2012), voltage controlled exchange energies of a two-electron silicon double quantum dot with and without charge defects in the dielectric.
- [28] N. Ikarashi and K. Watanabe, *Jpn. J. Appl. Phys.* **39**, 1278 (2000).
- [29] O. L. Krivanek and J. H. Mazur, *Appl. Phys. Lett.* **37**, 392 (1980).
- [30] W. R. Anderson et al., *Micro. Eng.* **22**, 43 (1993).
- [31] B. Weber et al., *Nature Nano.* **9**, 430 (2014).
- [32] J. R. Petta et al., *Science* **309**, 2180 (2005).
- [33] N. S. Lai et al., *Sci. Rep.* **1**, 110 (2011).
- [34] N. Shaji et al., *Nature Physics* **4**, 540 (2008).
- [35] J. K. Perron et al. (2016), unpublished.
- [36] K. Li et al., *J. Vac. Sci. Technol. B* **29**, 041806 (2011).
- [37] S. Tanaka et al., *Appl. Phys. Lett.* **69**, 1235 (1996).
- [38] B. G. Streetman, *Solid State Electronic Devices* (Prentice Hall, Englewood Cliffs, NJ, USA, 1995).

Supplementary Information on Whether the Electron Wavefunction Follows the Interface

In this Section, we will discuss this question as follows:

1. We will give a formal analysis, based on symmetry arguments, that yields the result that the wavefunction follows the interface for any interface slope less than one. This analysis is relevant for the smooth (Si/SiO₂) interfaces considered in this paper.
2. We will give an estimate based on energy considerations, that yields the result that the wavefunction follows the interface for any interface roughness with correlation length greater than about 0.3 nm. This analysis is relevant for both step (Si/SiGe) and smooth (Si/SiO₂) interfaces considered in this paper.
3. Based on the two analyses, we will present a result from our simulations where we compare the valley phase for i) an interface with vertical steps to ii) an interface with sloped steps, and show that the valley phase is approximately the same for both interfaces. This result shows that the formal analysis (item 1. above) is thus also relevant for the step (Si/SiGe interfaces).

A. Symmetry Arguments

The Schrodinger equation in the absence of interface roughness is

$$\left[-\frac{\hbar^2 \nabla^2}{2m} + V(\mathbf{r}) \right] \psi_{\text{ew}}(\mathbf{r}) = \varepsilon \psi_e(\mathbf{r}), \quad (9)$$

Thus, the second derivatives in the original coordinate system are approximately the same as those in the new system, if $\left| \frac{\partial z'}{\partial x, y} \right| \ll 1$. In this case, we can immediately see that $\psi_e(x, y, z) \approx \psi_{e,0}(x, y, z - \zeta(x, y))$. In summary, if the slope of any interface roughness is substantially less than one, the electron wavefunction will approximately follow the interface.

where ψ_e is the total electron wavefunction (represented as $L_z(x, y, z)$) in Equation 3 in the main text. The solution to this equation is $\psi_{e,0}(\mathbf{r})$, the solution for a flat interface.

We wish to examine the effect on ψ_e when the interface becomes rough, and in particular on the amount by which the spatial derivatives change. We can define new coordinates

$$\begin{aligned} x' &= x \\ y' &= y \\ z' &= z - \zeta(x, y). \end{aligned} \quad (10)$$

The differentials transform as

$$\begin{aligned} \frac{\partial \psi_e}{\partial x} &= \frac{\partial \psi_e}{\partial x'} \frac{\partial x'}{\partial x} + \frac{\partial \psi_e}{\partial z'} \frac{\partial z'}{\partial x} = \frac{\partial \psi_e}{\partial x'} + \frac{\partial \psi_e}{\partial z'} \frac{\partial z'}{\partial x} \\ \frac{\partial \psi_e}{\partial y} &= \frac{\partial \psi_e}{\partial y'} \frac{\partial y'}{\partial y} + \frac{\partial \psi_e}{\partial z'} \frac{\partial z'}{\partial y} = \frac{\partial \psi_e}{\partial y'} + \frac{\partial \psi_e}{\partial z'} \frac{\partial z'}{\partial y} \\ \frac{\partial \psi_e}{\partial z} &= \frac{\partial \psi_e}{\partial z'} \frac{\partial z'}{\partial z} = \frac{\partial \psi_e}{\partial z'}. \end{aligned} \quad (11)$$

The second differentials become

$$\begin{aligned} \frac{\partial}{\partial x} \frac{\partial \psi_e}{\partial x} &= \left(\frac{\partial}{\partial x'} + \frac{\partial z'}{\partial x} \frac{\partial}{\partial z'} \right) \left(\frac{\partial \psi_e}{\partial x'} + \frac{\partial \psi_e}{\partial z'} \frac{\partial z'}{\partial x} \right) = \left[\frac{\partial^2 \psi_e}{\partial x'^2} + 2 \frac{\partial^2 \psi_e}{\partial x' \partial z'} \frac{\partial z'}{\partial x} + \frac{\partial^2 \psi_e}{\partial z'^2} \left(\frac{\partial z'}{\partial x} \right)^2 \right] \\ \frac{\partial}{\partial y} \frac{\partial \psi_e}{\partial y} &= \left(\frac{\partial}{\partial y'} + \frac{\partial z'}{\partial y} \frac{\partial}{\partial z'} \right) \left(\frac{\partial \psi_e}{\partial y'} + \frac{\partial \psi_e}{\partial z'} \frac{\partial z'}{\partial y} \right) = \left[\frac{\partial^2 \psi_e}{\partial y'^2} + 2 \frac{\partial^2 \psi_e}{\partial y' \partial z'} \frac{\partial z'}{\partial y} + \frac{\partial^2 \psi_e}{\partial z'^2} \left(\frac{\partial z'}{\partial y} \right)^2 \right] \\ \frac{\partial}{\partial z} \frac{\partial \psi_e}{\partial z} &= \frac{\partial^2 \psi_e}{\partial z'^2}. \end{aligned} \quad (12)$$

B. Energy Considerations

Here, we consider the interplay between kinetic and potential energies. For a rough interface, since the accumulation gate produces a potential well in the z-direction at the interface and follows conformally the interface roughness, the electron potential energy will be lowered if the wavefunction follows the interface roughness exactly (Fig. S2). On the other hand, the more the wavefunction follows the interface roughness, the larger is the kinetic en-

ergy increase. For simplicity, we consider only one lateral direction x .

Thus, we determine the approximate maximum bending of the electron wavefunction by the constraint

$$\frac{\hbar^2}{2m} \frac{d^2 \psi_{\text{ew}}}{dx^2} < (\mathcal{V} + eFz) \psi_{\text{ew}} \quad (13)$$

in the effective mass approximation (EMA). Note that, for this inequality, the normalization of the wavefunction is present on both sides, so we will suppress the normalization factor.

We define the following parameters:

$\psi_{\text{ew}} = \phi(x, y) \psi(z)$ Electron envelope wavefunction in the EMA.

$\zeta_{\text{ew}}(\mathbf{x})$ Height of center of electron wavefunction (as distinguished from the height of the interface $\zeta(x)$). [See Figure 4]

ζ_{e0} Amplitude of local bending of electron wavefunction (assumed to be quadratic).

l_{ce} Correlation length of electron wavefunction (as distinguished from the correlation length of the interface).

U_0 Band offset between Si and SiO₂, as in Equation 5 of the main text.

t Vertical thickness of electron 2DEG (inversion layer thickness).

m Effective mass of transverse electron in Si; $m = 0.2m_e$.

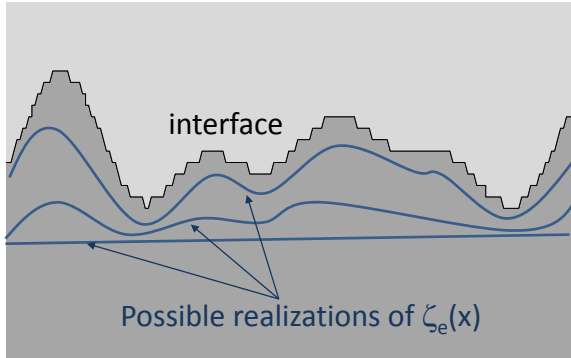


FIG. 4: Figure S1: Possible realizations of $\zeta_{\text{ew}}(\mathbf{x})$; the correct realization depends on the interplay between kinetic and potential energy. Bottom curve: kinetic energy term dominates; top curve: potential energy term dominates.

1. Kinetic Energy

To approximate the left-hand side of Equation 13, we start by assuming that the wavefunction is locally quadratic:

$$\zeta_{\text{ew}}(x) = (\zeta_{\text{e0}}) \left(\frac{x}{l_{\text{ce}}} \right)^2. \quad (14)$$

Following Equation 3 in the main text, the EMA envelope wavefunction is

$$\psi_{\text{ew}}(x, z) = \phi_D(x) \psi(\zeta_{\text{ew}}(x) - z). \quad (15)$$

A good approximation to the z -dependence of the 2DEG is $\psi(x, z) = e^{-(\zeta_{\text{ew}}(x)-z)/t}$ (ref [38]). The contribution to the kinetic energy from the roughness of the 2DEG comes only from this part of the total wavefunction $\psi_{\text{ew}}(x, z)$:

$$\frac{d^2 \psi_{\text{ew}}}{dx^2} = \psi_{\text{ew}} \left[\left(\frac{\zeta_{\text{ew}}'}{t} \right)^2 - \frac{\zeta_{\text{ew}}''}{t} \right]. \quad (16)$$

With the quadratic dependence of $\zeta_{\text{ew}}(x)$, and evaluating at $x = l_{\text{ce}}$, we obtain

$$\frac{d^2 \psi_{\text{ew}}}{dx^2} \approx \psi_{\text{ew}} \left(2 \frac{\zeta_{\text{e0}}}{l_{\text{ce}} t} \right)^2 \left[1 - \frac{t}{2\zeta_{\text{e0}}} \right]. \quad (17)$$

With $t/\zeta_{\text{e0}} \approx 5 \text{ nm} / 0.5 \text{ nm}$,

$$\frac{d^2 \psi_{\text{ew}}}{dx^2} \approx \psi_{\text{ew}} \left(-2 \frac{\zeta_{\text{e0}}}{l_{\text{ce}}^2 t} \right). \quad (18)$$

Finally, the left hand side of Equation 13 is

$$\frac{\hbar^2}{2m} \frac{d^2 \psi_{\text{ew}}}{dx^2} \approx \psi_{\text{ew}} \left(-\frac{\hbar^2}{m} \frac{\zeta_{\text{e0}}}{l_{\text{ce}}^2 t} \right). \quad (19)$$

2. Potential Energy

We approximate the vertical potential well at the interface as triangular, with the sloped section having a slope of U_0/t . The decrease in potential energy when the electron wavefunction is bent with a vertical change of approximately ζ_{e0} instead of flat is thus

$$(\mathcal{V} + eFz) \psi_{\text{ew}} \approx \psi_{\text{ew}} \frac{U_0 \zeta_{\text{e0}}}{t}. \quad (20)$$

3. Summary

Combining Equations 13, 19, 20, we thus obtain a constraint on the minimum radius of curvature or correlation length of the electron wavefunction

$$l_{ce}^2 > \frac{\hbar^2}{mU_0}; \quad (21)$$

using the values in this section ($U_0 = 3$ eV for Si/SiO₂), we finally obtain $l_{ce} > \approx 0.3$ nm. Given that the typical amplitude of roughness is less than or of order 1 nm, this condition is quite similar to that in the previous argument based on symmetry considerations.

C. Results from Simulations

Figure 5 shows two choices for $\zeta_{ew}(x)$, with the smoothed one obeying the approximate constraints derived in the last two sections. We simulated the phase difference, and got the result

$$\Delta\phi_{sharp} = -0.110(2\pi), \Delta\phi_{smoothed} = -0.111(2\pi). \quad (22)$$

Thus, the results of a combination of i) two theoretical constraints on the sharpness of the electron wavefunction as viewed through $\zeta_{ew}(x)$, and ii) the very small phase difference for the sharp versus smoothed electron wavefunctions, demonstrate that our assumption in the main text (that the electron wavefunction follows the interface roughness) does not present a significant offset in our results.

D. Using only the Ground Orbital State

In this section, we give the assumption underlying the use of only the ground orbital state, and discuss the plausibility of this assumption.

For a flat interface, we can identify the eigenstates as $|\lambda z\rangle = \phi_\lambda(x, y) \psi(z) u_z(\mathbf{r}) e^{ik_0 z}$, following Equation 3 in the main text. Here, λ is the orbital state index, and z, \bar{z} are the two possible valley states.

For the full treatment of the rough interface, we would consider a potential $V = V_{flat} + \Delta V$, where V_{flat} is the potential in Equation 5 in the main text, and ΔV is a perturbation on the flat interface potential. In this case, in order to calculate the full eigenstates, we would consider Hamiltonian matrix elements $\langle \lambda z | \Delta V | \lambda' \bar{z} \rangle$, including intra-valley intra-orbital, intervalley intra-orbital, and intervalley inter-orbital terms. The first two types of terms, while leading to mixing of the orbital states, will not affect our results for the valley phase.

However, the last term (intervalley and inter-orbital) will affect, and in particular will likely make substantially smaller through statistical averaging, the valley phase.

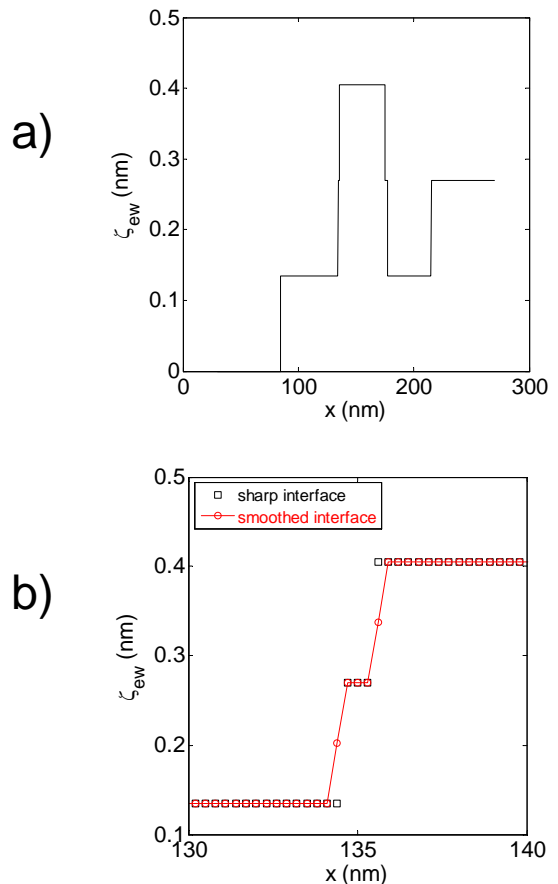


FIG. 5: Figure S2: Sharp and smoothed vertical centers $\zeta_{ew}(x)$ of electron wavefunction, for testing dependence of $\Delta\phi$ on the extent to which electron wavefunction follows interface roughness. a) Full extent of sharp $\zeta_{ew}(x)$ for Si/SiGe simulated interface; quantum dots are centered at 125 and 175 nm, with dot radius $a = 10.4$ nm; b) Small region of interface, showing smoothing of the original sharp $\zeta_{ew}(x)$ to give a slope less than one, or a correlation length greater than 0.3 nm.

The relevant parameter that determines the level of intervalley interorbital mixing is $\beta = \frac{\langle \lambda z | \Delta V | \lambda' \bar{z} \rangle}{E_\lambda - E'_\lambda}$.

Thus, the assumption underlying the use of only the ground orbital states is that $\beta \ll 1$. There are two arguments for believing that this approximation is justified:

1. Theoretical estimate: The numerator of β is apparently less than the valley splitting $\langle \lambda z | \Delta V | \lambda' \bar{z} \rangle$, where $|\lambda z\rangle$ is the ground orbital state. Since the valley splitting gets smaller as the interface roughness increases, while the orbital energy splitting stays the same, it appears that β will be substantially less than one for a rough interface.
2. Experimental: In terms of results for both magnitude of valley splitting and orbital energy splitting we can point to one group which has measured the

valley splitting to be between 0.3 and 0.8 meV[7] and the orbital energy splitting to be as large as 8 meV[7].

E. Files

All pathnames are relative to
L:/internal/SET_team/Neil/other peoples documents/Culcer/valleys 14.5

Text: /manuscript/text/Culcer_valley_phase_v_2.tex.

All figures /manuscript/figures/15_11 portrait Culcer phase figures.pptx.

Fig 1 Main: /manuscript/figures/Delta phi plots/Step_NonVicinal.dat and Step_Vicinal.dat

using do_plot_step_vicinal.m.

Fig 2 Main: /manuscript/figures/Delta phi plots/Sin_NonVicinal.dat and Sin_Vicinal.dat using do_plot_sin_vicinal.m.

Fig 3 both panels manuscript/figures/voltage control/VoltageControl_XL10.dat and _XL0.dat using do_plot_voltage_control.m.

Fig S1 /manuscript/figures/15_11 portrait Culcer phase figures.pptx.

Fig S2 /manuscript/figures/smoothed for Supp/xi_x_steps_tilt_0_rand_1.dat, using do_plot_smoothed_unsmoothed.m, followed by xli, cla, plot(x, y, 'k-')